ELSEVIER

Polymer Vol. 37 No. 10, pp. 1857–1870, 1996

0032-3861/96/$15.00+0.00

Extracting force fields for disordered polymeric materials from neutron scattering data

Barbara Rosi-Schwartz and Geoffrey R. Mitchell*
Polymer Science Centre, J.J. Thomson Physical Laboratory, University of Reading, Whiteknights, Reading RG6 6AF, UK
(Revised 5 September 1995)

We present a new approach that allows the determination of force-field parameters for the description of disordered macromolecular systems from experimental neutron diffraction data obtained over a large Q range. The procedure is based on a tight coupling between experimentally derived structure factors and computer modelling. We separate the molecular potential into non-interacting terms representing respectively bond stretching, angle bending and torsional rotation. The parameters for each of the potentials are extracted directly from experimental data through comparison of the experimental structure factor and those derived from atomistic level molecular models. The viability of these force fields is assessed by comparison of predicted large-scale features such as the characteristic ratio. The procedure is illustrated on molten poly(ethylene) and poly(tetrafluoroethylene). Copyright © 1996 Published by Elsevier Science Ltd.

(Keywords: force-field parameters; disordered materials; neutron diffraction data; molecular modelling)

INTRODUCTION

In the past few years we have seen a considerable growth of interest in the predictive modelling of synthetic polymers, undoubtedly due both to rapid developments of simulation techniques and to the extensive availability of computer resources, which offer the possibility of performing quantitative molecular dynamics and Monte Carlo simulations of large macromolecular systems.

Whilst molecular liquids can normally be described in terms of short-range interactions and short-time fluctuations, the complexity and connectivity of macromolecular systems make it necessary to take into consideration interactions over a very wide range of length and time scales. A simplifying approach to this complex task involves removing all of the chemical detail in the description of the polymer chain and using a freely jointed bead model to treat the chain interactions, each bead representing a statistical unit in the chain[1]. This type of approach, frequently coupled with the positioning of the chain onto a lattice[2], has borne very fruitful results in terms of the study of long-range interactions and long-time diffusive behaviour of molten and glassy polymer systems[3,4]. The main shortcoming of the models produced by these techniques is their lack of information on the conformations of realistic chains, an obvious consequence of the simplifying assumptions made in these approaches. Yet it is the detailed chain conformational features of the polymeric chain that determine many of the relevant properties of the material, such as mechanical, optical and electrical characteristics.

More detailed atomistic modelling approaches, utilizing both molecular mechanics (MM)[5,6] and molecular dynamics (MD)[7,8] techniques, have been proposed in the past few years. In general, in these approaches, the chain conformation is described in terms of two-, three- and four-body intramolecular potentials relating to bond stretching, valence angle bending and dihedral rotations respectively. Non-bonded contributions to the intramolecular potential are generally represented through van der Waals and electrostatic interactions. It is generally recognized that the reliability of the simulations is ultimately determined by the quality and accuracy of the force fields employed, and as a consequence of this a number of investigators have turned their attention to force-field development specific to polymeric materials[9,10]. Various force fields have been proposed to date, expressing the intramolecular potentials in analytical forms that are dependent upon a number of 'empirical' parameters describing the detailed shape of the potentials. Whilst these force fields are tested whenever possible by a comparison of predicted properties of the materials with experimental values, the fact that such force fields have been mostly obtained by either *ab initio* calculations or experiments on small molecules is a possible shortcoming of these potentials, as they do not necessarily provide a sufficiently accurate description of such systems as complex as polymeric materials. This is particularly true in the case of polymers with 'unusual' chemical configurations or those with long-range electrostatic intrachain interactions. In fact, we have recently shown that, in the case of fluorinated polymers, most of the available force fields fail to predict the correct chain conformation for the crystalline

* To whom correspondence should be addressed

structure[11,12], which has been determined by X-ray diffraction experiments[13,14]. That work has shown that the accurate reproduction of properties of the real system is crucially dependent on the detailed form chosen for the intramolecular potential.

Hence the need arises for a direct way of testing and validating force-field expressions and related parameters for an accurate description of macromolecules. Once validated, such force fields could be used for various types of simulations to predict various properties of the materials of interest.

In this contribution we describe an exploratory study of a novel approach that allows the *experimental* determination of intramolecular potentials suitable for polymer glasses and melts. The study is made possible by the availability of diffraction data over a very wide Q range ($|Q| = 4\pi \sin\theta/\lambda$), and therefore of high-resolution distribution functions in real space, as offered by state-of-the-art pulsed neutron sources. By expressing a model single chain as a function of a number of geometric and conformational parameters, and by systematically varying these parameters to minimize the difference between predicted structure factor and experimental data, it is possible to obtain information on the detail of the force-field term relevant to each structural parameter.

Conventionally force fields are tested through the prediction of the minimum-energy structure of the material of interest, for example, molecular structures obtained from crystallographic studies. However, the validation of several force-field parameters through a single structure is somewhat ambiguous. Highly disordered polymer structures such as melts exhibit configurations that are characterized by significant populations of high-energy states. This is most apparent in a consideration of the torsional angle distribution for skeletal bonds, and it is this local scale of structure that can be directly accessed through broad-Q neutron scattering. Thus polymer melts are equilibrium structures, which are advantageous in this respect in that they offer an array of observable local structures against which the force-field expressions can be tested.

We will contrast results obtained in the exploratory study on molten poly(ethylene) (PE) and molten poly(tetrafluoroethylene) (PTFE); although similar in their chemical structure, these polymers are characterized by profoundly different properties arising from their different chain conformations. Whilst force-field expressions have been proposed in the literature for alkane molecules[15-18], the information specific to PTFE or oligomers is scarce. This comparison of PE and PTFE will show the sensitivity of broad-Q neutron scattering to the details of the expressions describing the force fields; although preliminary and therefore approximate, the results we report indicate that this approach indeed constitutes a new way forward to the determination and validation of viable force-field expressions for non-crystalline polymers.

METHODOLOGY

Our approach is based on the observation that the structure factor $S(Q)$ is dominated by intrachain correlations in the region $Q > 2\,\text{Å}^{-1}$ (refs 19, 20). The lower-Q region ($0.5 < Q < 2\,\text{Å}^{-1}$) arises predominantly from the interchain structure. Therefore information on intramolecular potentials can be extracted from the experimental results by limiting the analysis of the structure factor to the intrachain part of the diffraction pattern. As previously mentioned, the availability of diffraction data over a very wide Q range makes the analysis very accurate and detailed.

The intrachain structure can be described by the chemical topology and by the definition of potential functions for bond lengths, bond angles and torsional angles. For a given chain molecule there will be sets of chemically equivalent bond lengths, bond angles and torsional angles. In other words, for a particular polymer, only a relatively small number of potential functions will be required. In the case of PE, we will need two bond length potentials, three bond angle potentials and one torsional potential. In this work we have considered these potentials as independent non-interacting elements, and hence the total energy E is given by:

$$E = \sum E_{\text{bond}} + \sum E_{\text{angle}} + \sum E_{\text{torsional}} \qquad (1)$$

The independence of the energy terms allows us to factorize the partition function Z into a set of equivalent terms, and thus the probability distribution for any structural component (i.e. bond length, bond angle or torsional angle) may be obtained directly. Here we give, as an example, the probability distribution $p(l)$ for the l_{C-C} bond length:

$$p(l)_{l_{C-C}} = \frac{\exp(-E_{l_{C-C}}/RT)}{\sum \exp(-E_{l_{C-C}}/RT)} \qquad (2)$$

where the partition function is summed only over possible values of l_{C-C}.

The particular values for each set of bond lengths, bond angles and torsional angles can now be set by random sampling procedures. These sampling methods ensure that the distribution of chemical equivalent bond lengths, etc., for a particular chain reflects the calculated probability distributions. Atomistic level molecular models can then be built using the particular values assigned to each bond length, bond angle and torsional angle.

It is sometimes the case that the energy function for a particular torsional angle depends significantly upon its environment. In this exploratory work we have used independent potentials, which lead to probabilities that are not dependent on the nature of preceding or following torsional states. This is not an intrinsic limitation of the procedure described here. Once the model is built and the Cartesian coordinates for all atoms are known, it is straightforwarward to calculate the static structure factor that is to be expected from such a model[20]. This can then be quantitatively compared with the equivalent experimentally derived function through the following χ^2 test:

$$\chi^2 = \frac{1}{n_Q} \sum_{i=1}^{n_Q} [Q_i S_C(Q_i) - Q_i S_E(Q_i)]^2 \qquad (3)$$

where n_Q is the number of Q points in the scattering curve and S_E and S_C are the experimental and calculated structure factors respectively[11]. By systematically searching through the various force-field parameter spaces, the global minimum in χ^2 can be identified, which represents the most appropriate expression for the intrachain potential for the system of interest.

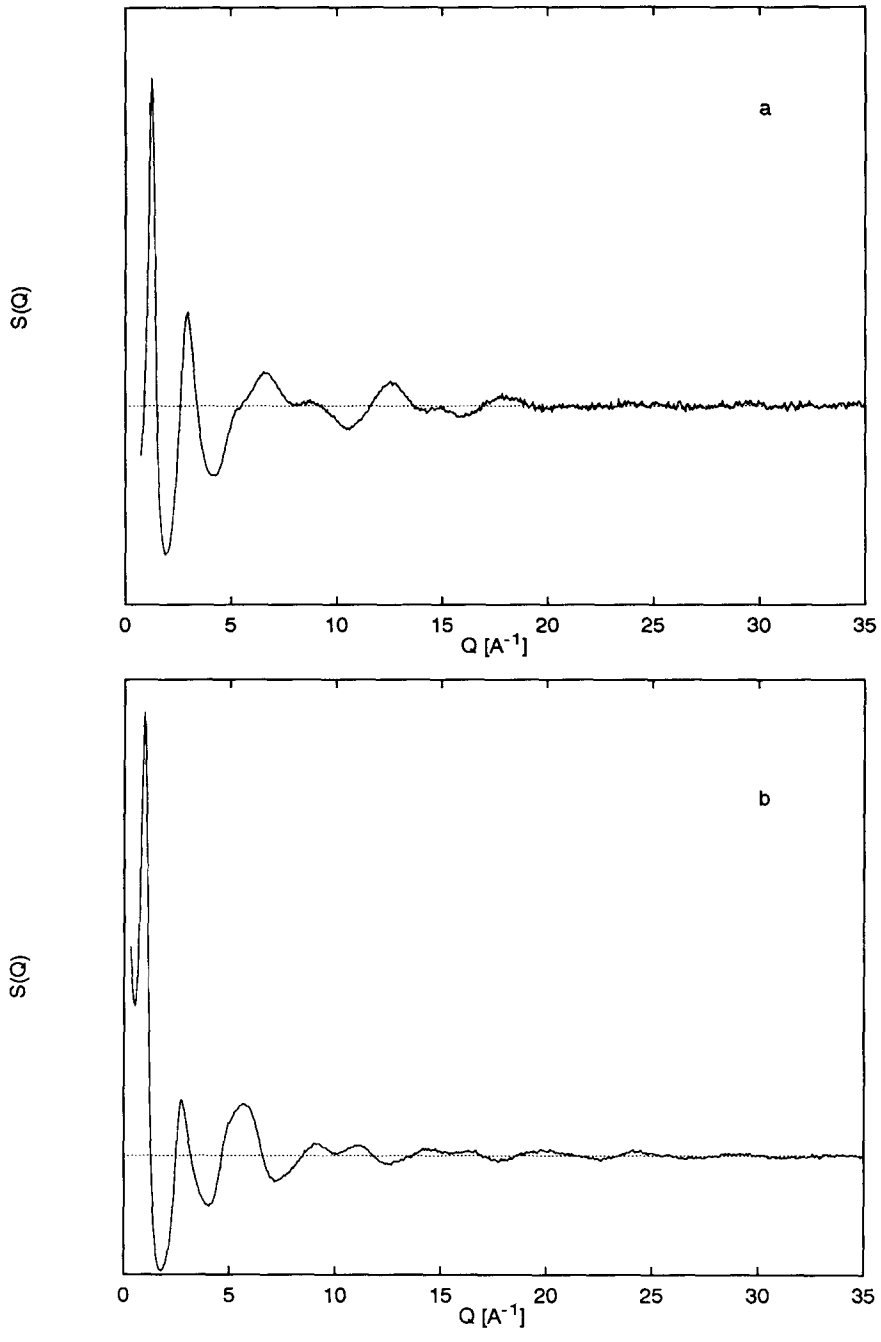

Figure 1 Experimental $S(Q)$ for (a) PE at $T = 150°C$ and (b) PTFE at $T = 350°C$, after data correction and normalization[11,22]

Owing to the statistical nature of the real structure, the calculated structure factor needs to be obtained from a model large enough to be fully representative in terms of the distributions of each parameter and in terms of the structure factor. In the work described here, we have averaged the results from a standard model of 15 000 atoms, which gives a contour length of the chain of more than 6000 Å. We have performed extensive tests to determine the extent of averaging required, and as a consequence we have used 100 models in terms of torsional angle distributions, two models in terms of bond length distributions and 10 models in terms of bond angle distributions. We have used unbiased distributions of these intrachain structural parameters to generate each polymer model, which was, therefore, not a self-avoiding configuration. To avoid the inclusion of unrealistic interchain-type correlations in the scattering calculations, a window is placed on the length of chain considered at any one time, typically ~ 20 skeletal bonds[20].

These calculations have been performed with a comprehensive software package developed at Reading, MESA (Molecular Editor for Structural Analysis), which is specifically tailored to this type of investigation[21]. In order to find the set of force-field parameters that generate chain conformations exhibiting a structure factor in best agreement with the observed structure factor, we have searched systematically through the complete parameter space. We have used a variable-sized grid scan coupled with the Ravine procedure in order to ensure that the global minimum is found.

In this work we have utilized neutron scattering

data for PE and PTFE obtained from some of our previous studies[11,22], and *Figure 1* shows the structure factors $S(Q)$ obtained after data correction and normalization.

We will further evaluate the force fields derived in this work by calculating larger-scale properties than the structure factor. In particular, we will present values of the persistence length q and the characteristic ratio C_∞, defined as $\langle r^2\rangle_0/nl^2$, where $\langle r^2\rangle_0$ is the unperturbed mean-square end-to-end length, n is the number of skeletal bonds and l is the bond length. These were obtained using the same procedures as described above to generate atomistic models, from which simple geometry yielded both the end-to-end length r^2, the radius of gyration r_g^2 and the persistence length q, as a function of the number of skeletal bonds. By averaging over typically 5000 models, the asymptotic values of both properties in the infinite-chain limit could be obtained.

RESULTS AND DISCUSSION

Figure 2 shows a sketch of the relevant structural parameters used in our refinement procedure. We have chosen harmonic potentials for the bond length stretching and valence angle bending potentials[23,24]. The torsional potential was treated using two different analytical forms. Each of the terms will now be discussed in turn.

The bond stretching term for both the C–C and C–X bonds, where X = D (PE) or X = F (PTFE) respectively, was assumed to be of the following form:

$$E_s(l) = K_s(l - l_0)^2 \qquad (4)$$

where K_s is the stretching force constant and l_0 is the mean bond length. Using these energy functions and the temperature of the system T, a set of probability distribution functions can be obtained and used to assign the bond lengths to a particular chain as described in the preceding section. The force-field parameters l_0 and K_s were evaluated using the search procedure described above. One advantage of the grid scan search method is that we can observe directly the sensitivity of the structure factor through the χ^2 test to particular force-field parameters. *Figure 3* shows an example of the results obtained, in this case for PTFE. As can be clearly seen, a minimum in the χ^2 surface can be unambiguously identified. Whilst some previous MD studies on alkane molecules have neglected the bond stretching term owing to the very high frequency of the stretching motions and their decoupling from the other slower molecular degrees of freedom[17,25], our χ^2 test indicates that the introduction of harmonic distributions for both the C–C and C–X bonds improves considerably the fit to the experimental structure factor with respect to the case of rigid bonds.

The parameter values for the potential term of equation (4) at the absolute minimum are summarized in *Tables 1* and *2* for PE and PTFE respectively, together with a comparison with the values utilized in the CHARMm[26], AMBER[27] and CFF91[28] force fields. There are no specific parameters given for deuterium as distinct from hydrogen in these published parametrizations, and so we have compared where appropriate with the values for hydrogen. The values we obtain for the mean backbone bond length and valence angle are consistent, within experimental error, with values determined from X-ray scattering investigation on a series of liquid alkane molecules[29]. A neutron scattering experiment on molten deuterated PE[30], on the other hand, provides mean values for bond lengths and bond angles that are slightly different from the ones obtained in this work. This

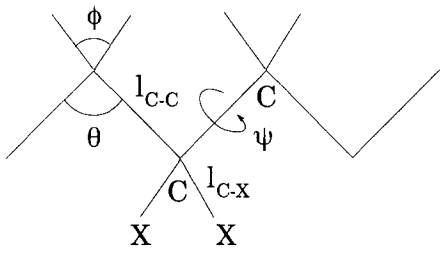

Figure 2 Schematic representation of a chain segment and of the relevant structural parameters

Table 1 Optimized bond length parameters obtained in this work on molten PE. As a comparison, the values utilized by the CHARMm, AMBER and CFF91 force fields are also reported

	l_0(C–C) (Å)	K_s(C–C) (kcal mol^{-1} Å^{-2})	l_0(C–D) (Å)	K_s(C–D) (kcal mol^{-1} Å^{-2})
Our procedure	1.56 ± 0.01	250 ± 50	1.12 ± 0.01	113 ± 50
CHARMm[26]	1.529	268.00	1.090	340.00
Amber[27]	1.526	310.00	1.090	331.00
CFF91[28]	1.526	322.72	1.105	340.62

Table 2 Same as *Table 1*, but for molten PTFE

	l_0(C–C) (Å)	K_s(C–C) (kcal mol^{-1} Å^{-2})	l_0(C–F) (Å)	K_s(C–F) (kcal mol^{-1} Å^{-2})
Our procedure	1.59 ± 0.01	149 ± 50	1.35 ± 0.01	476 ± 50
CHARMm	1.512	298.00	1.335	275.00
Amber	1.526	310.00		
CFF91	1.526	322.72	1.363	496.00

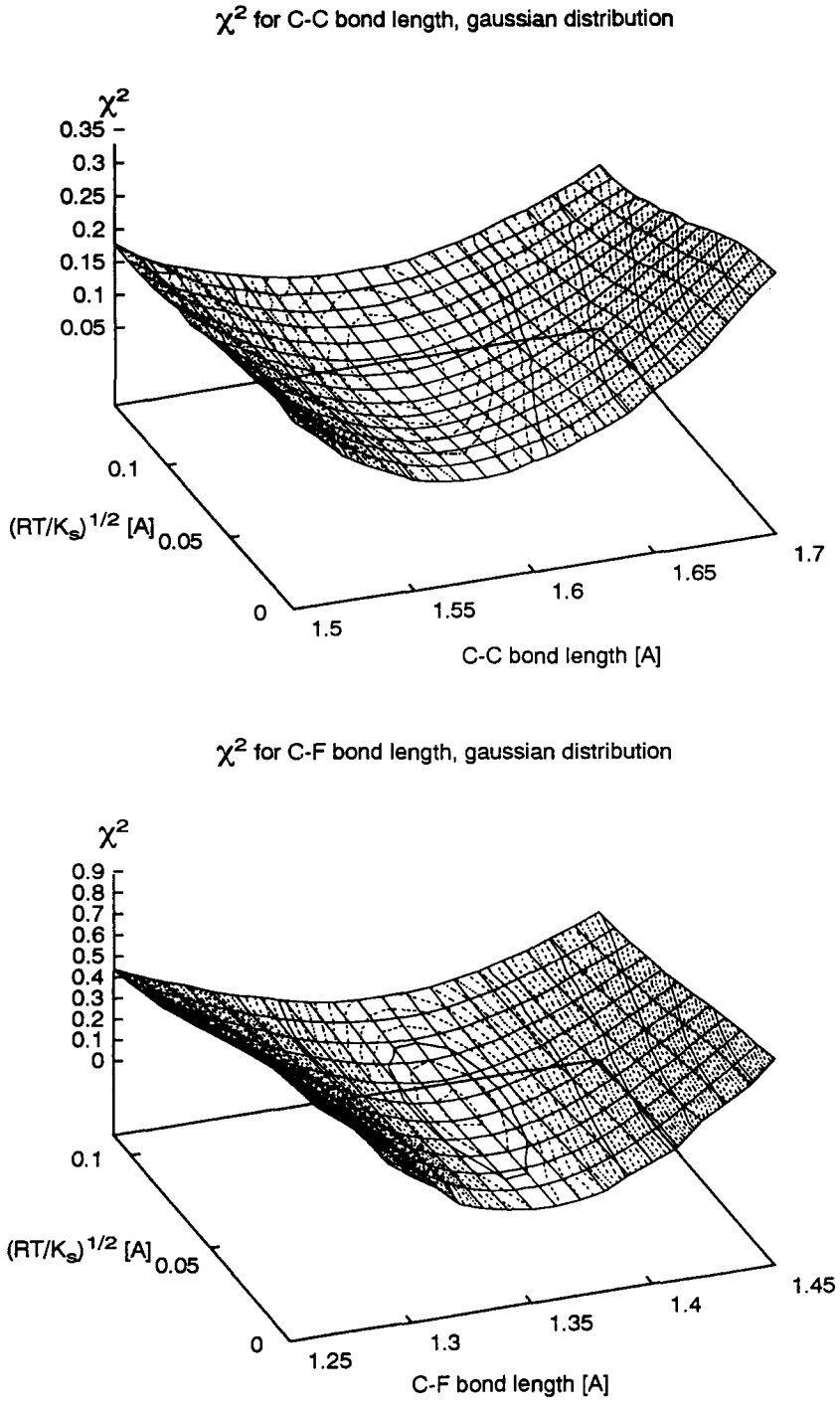

Figure 3 Determination of the bond stretching force field for (a) C–C and (b) C–F bond for PTFE. The χ^2 behaviour is represented as a function of peak position and width of the assumed Gaussian distribution

might be connected with the more simplified model used by Misawa *et al.* to extract the geometric parameters from a fit of the experimental results, since the parameters are considered rigid. It should be noted that the values given in these tables are the result of a complete optimization of all the force-field parameters including those described in later sections. We present the individual force-field terms sequentially for clarity.

Clearly there are differences between these various sets of force-field parameters, most notably in the case of PTFE. For PTFE, the most probable C–F bond length distribution is somewhat narrower than that displayed for the C–C bond length distribution. This may be related to the great electrostatic interactions of the atoms in the side bonds. Furthermore, the considerable lengthening of the C–C equilibrium bond length, which in most studies is assumed to be 1.54 Å, is also a consequence of the repulsive interaction of the fluorine side groups.

For PTFE we have also considered an additional term to the bond stretching force field, namely anharmonicity in the potential term for the C–F bond. We have introduced a third-power term in the harmonic potential:

$$E_{s_{C-F}}(l) = K_{s_{C-F}}(l - l_0)^2 + K_{as_{C-F}}(l - l_0)^3 \qquad (5)$$

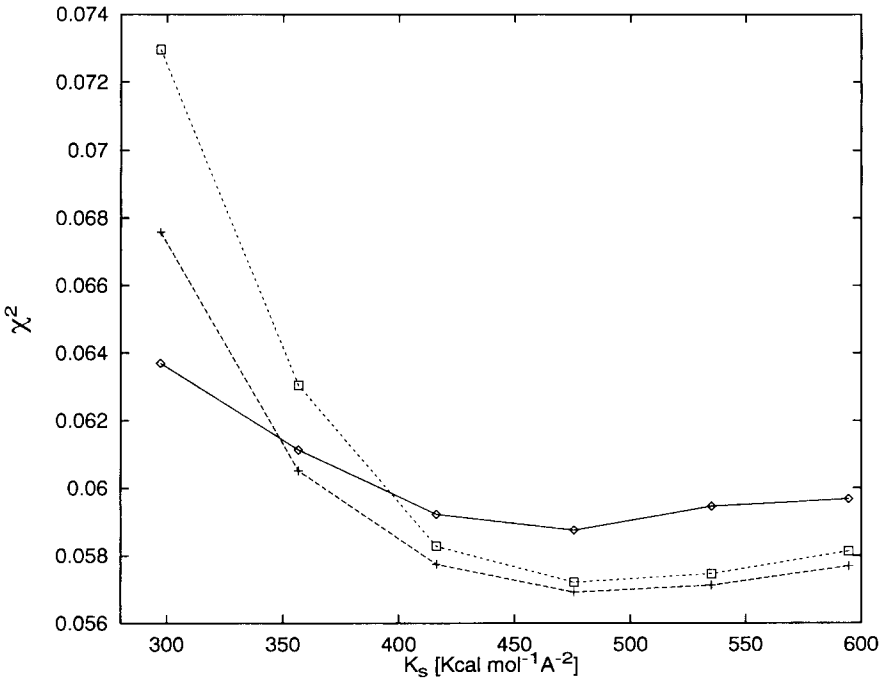

Figure 4 Plots of χ^2 vs. harmonic term force constant K_s in the C–F bond potential for PTFE, for three different values of the anharmonic term force constant K_{as}: (◇) $K_{as} = 0$ kcal mol^{-1} Å^{-2}; (+) $K_{as} = 1000$ kcal mol^{-1} Å^{-2}; and (□) $K_{as} = 1500$ kcal mol^{-1} Å^{-2}

and we have determined the corresponding force constant. *Figure 4* shows the behaviour of χ^2 as a function of the harmonic force constant K_s, for three different values of the anharmonic force constant K_{as}. As can be seen, the quality of the fit to the experimental structure factor improves for $K_{as}/K_s \approx 2$, although as might be expected the sensitivity is fairly low. Similar values were obtained from independent semiempirical molecular orbital calculations (MOPAC)[31] performed by us. *Figure 5* shows the behaviour of the heat of formation H_f calculated, using MOPAC, for a fragment of PTFE chain with stretching of the C–F bond. The anharmonicity of the curve is evident. A fit of this curve with the same anharmonic function in equation (5) produced values for the corresponding parameters whose ratio was in good agreement with that obtained by the χ^2 minimization approach. It is clear from an examination of the two curves in *Figure 5* that the anharmonicity will only be observed where there is a significant fraction of bonds in the higher-energy states. The fact that we can make a reasonable assessment of the third parameter underlines the utility of highly disordered polymer structures in this type of procedure.

The function shown in equation (6) was used to represent the valence angle bending potential term, both for the backbone angle θ and for the side-group angle ϕ (as indicated in the sketch of *Figure 2*):

$$E_b = K_b(\theta - \theta_0)^2 \qquad (6)$$

where K_b is the angle bending force constant and θ_0 is the mean valence angle value. Following the same procedure outlined for the bond stretching term, the values for the parameters in equation (6) were extracted from the experimental structure factor. The results are summarized in *Tables 3* and *4* for PE and PTFE respectively. A

Table 3 Optimized bond angle parameters obtained in this work on molten PE. As a comparison, the values utilized by the CHARMm, AMBER and CFF91 force fields are also reported

	θ_0 (deg)	$K_b(\theta)$ (kcal mol^{-1} rad^{-2})	ϕ_0 (deg)	$K_b(\phi)$ (kcal mol^{-1} rad^{-2})
Our procedure	113 ± 1	28 ± 10	109 ± 1	6 ± 3
CHARMm	112.70	58.35	107.80	33.00
Amber	109.50	40.00	109.50	35.50
CFF91	112.67	39.516	107.66	39.641

Table 4 Same as *Table 3*, but for molten PTFE

	θ_0 (deg)	$K_b(\theta)$ (kcal mol^{-1} rad^{-2})	ϕ_0 (deg)	$K_b(\phi)$ (kcal mol^{-1} rad^{-2})
Our procedure	114 ± 1	83 ± 40	110 ± 1	176 ± 50
CHARMm	112.70	58.00	109.47	110.00
Amber	109.50	40.00		
CFF91	112.67	39.51	107.80	95.00

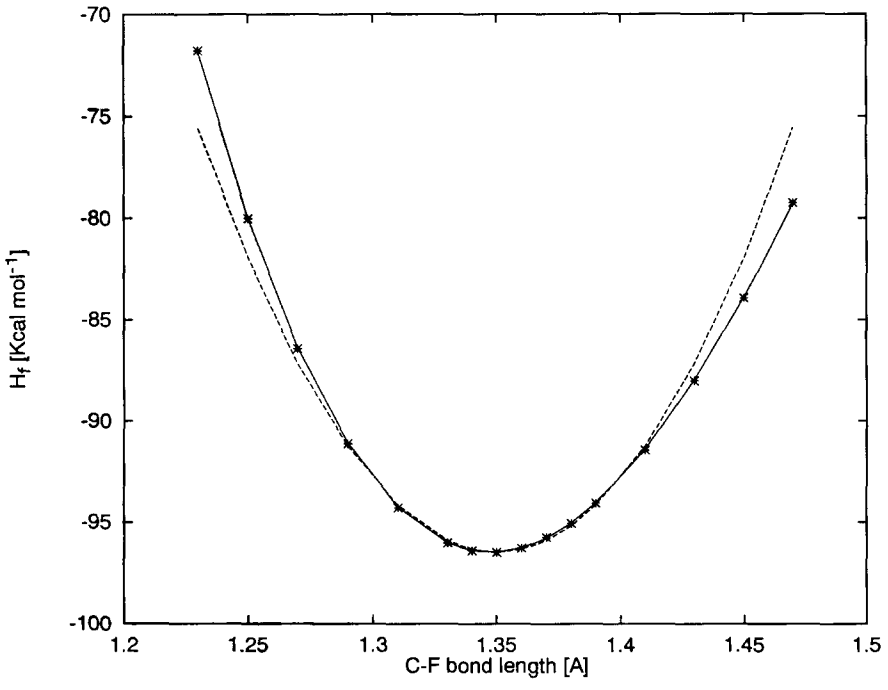

Figure 5 Heat of formation H_f vs. C–F bond length derived from semiempirical molecular orbital calculations on a fragment of PTFE chain. Symbols, results of the calculation; broken curve, fit with a harmonic expression; full curve, fit with an anharmonic expression

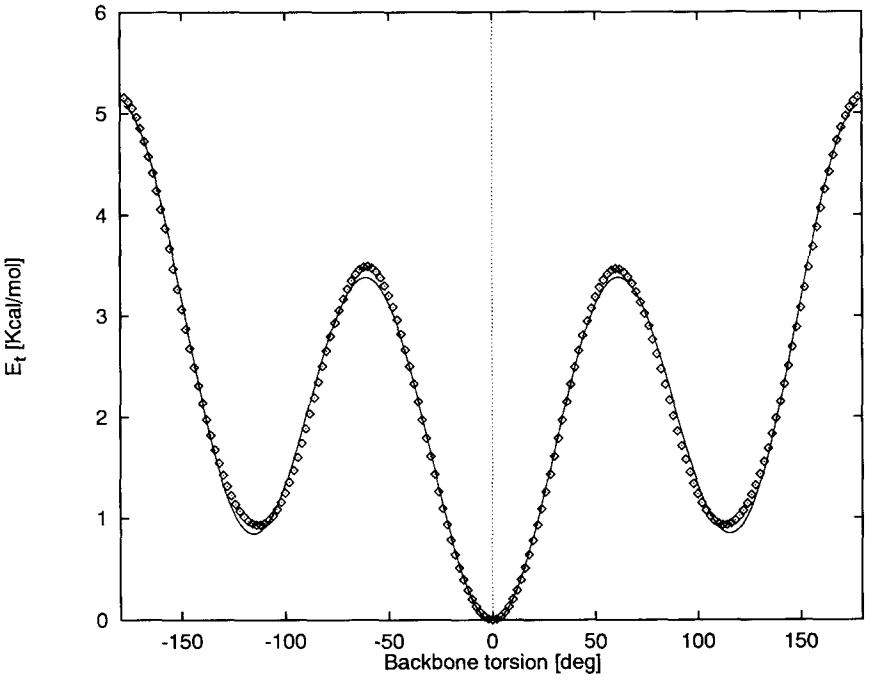

Figure 6 CHARMm energy vs. backbone torsional angle for a PE fragment. Symbols, the results of the CHARMm calculation; full curve, fit with a cosine power expansion

comparison of the constants shown for the different sets of force fields reveals a similar pattern to that shown for the bond stretching terms. Clearly a realistic force field is expected to predict not only the correct static structural features of the system, but also its dynamic properties. For this purpose we are currently testing the consistency of the force constants obtained with our refinement procedure with vibrational dynamics data obtained on the same sample.

As for the torsional potential, we will describe the procedure followed for the two polymers separately. Throughout this work we have adopted the convention that the torsional angle corresponding to the *trans* conformer has a value of 0°.

In the case of molten PE, the chosen form of the torsional potential follows the form of parametrization performed for n-alkanes by Steele[15], which was based on a combination of *ab initio* calculations and experimental data. Although in the past some extent of coupling between valence angle bending and torsional potential

has been suggested for n-alkanes[23], in most simulations the two terms have been kept separate and independent. We have made the same choice.

Preliminary calculations using the CHARMm force field[26] gave a variation of the total energy of the system with torsional angle as indicated in *Figure 6*. This curve was obtained by selecting a backbone torsion in the central part of a PE chain fragment of 12 alkyl units, varying the value of that torsional angle in regular steps, and at each step modifying the remaining geometry to minimize the energy of the fragment. The energy curve was then fitted with several functional forms, the most suitable of which was found to be a cosine power expansion similar to that employed by Steele *et al.*[15]; the full curve in *Figure 6* indicates the fit obtained. We found that four terms in the series were sufficient to describe the details of the energy curve. We therefore chose to utilize the same analytical function to describe the torsional potential:

$$E(\psi)_t = \sum_{i=0}^{3} c_i \cos^i(\psi) \qquad (7)$$

We utilized the same grid scan technique detailed above to determine the coefficients in this expansion appropriate to the PE melt data. The grid scan was made over an extensive range in terms of each coefficient. *Table 5* summarizes the values for the expansion coefficients that corresponded to a minimum in χ^2, together with the results obtained from the fit to the CHARMm energy curve and the values proposed by Steele in the case of n-butane[15]. It is important to note that the torsional potential obtained in this work is a complete potential, including those contributions conventionally considered separately as non-bonded and electrostatic interactions. In other words, the potential derived in this work expresses the overall environment in which the single model chain is embedded.

Table 5 Optimized torsional potential parameters obtained in this work on molten PE. As a comparison, the values obtained from a fit of the CHARMm energy and the values reported in the literature are indicated

	c_0 (kcal mol^{-1})	c_1 (kcal mol^{-1})	c_2 (kcal mol^{-1})	c_3 (kcal mol^{-1})
Our refinement	1.7	7.6	0.5	−11.5
CHARMm	2.0	4.2	0.5	−6.7
Steele[15]	2.1	4.3	1.2	−7.6

Figures 7 and *8* show the optimized torsional potential obtained in this work for PE and the corresponding distribution of torsional angles respectively. As can be seen, the potential is consistent with a three-states RIS (rotational isomeric states) style model: a Gaussian fit to the distribution of *Figure 8* gives the values of 0° for the *trans* state and ±117° for the two *gauche* states. The integrated intensities of the three Gaussian components provide a probability of *trans* torsions of 0.64, in agreement with previous RIS model-based results [22,32,33]. However, the breadth of the maxima in the probability distribution about the *trans* and *gauche* isomer positions emphasizes the importance of including such fluctuations in any realistic model of the local conformation as previously explored by Cook *et al.*[34,35] and earlier X-ray scattering-based studies[36].

We have finally proceeded to the calculation of larger-scale properties based on the force fields obtained in this work. We have estimated the characteristic ratio C_∞ for molten PE and its behaviour as a function of temperature. *Figure 9* shows the results obtained in this work for this parameter, whilst *Figure 10* shows a comparison of our results with the established values obtained from dilute-solution measurements[32] and confirmed for the melt using small-angle neutron scattering on labelled mixtures[37]. In *Figure 10* we have also displayed the values for C_∞ obtained from both a model proposed by Flory[32] and a recent Monte Carlo study of the conformational characteristics of isolated

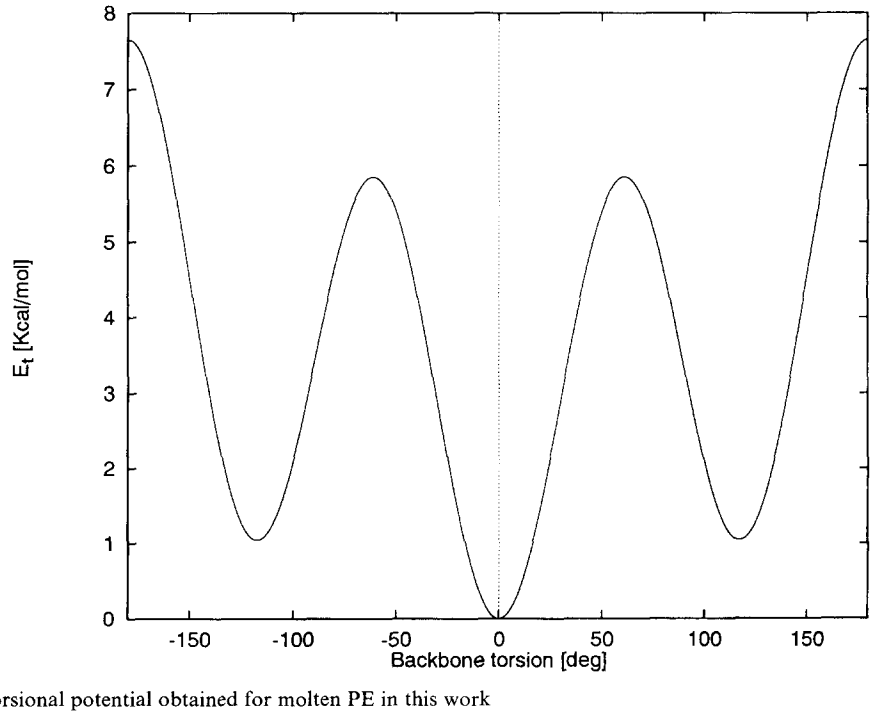

Figure 7 Optimized torsional potential obtained for molten PE in this work

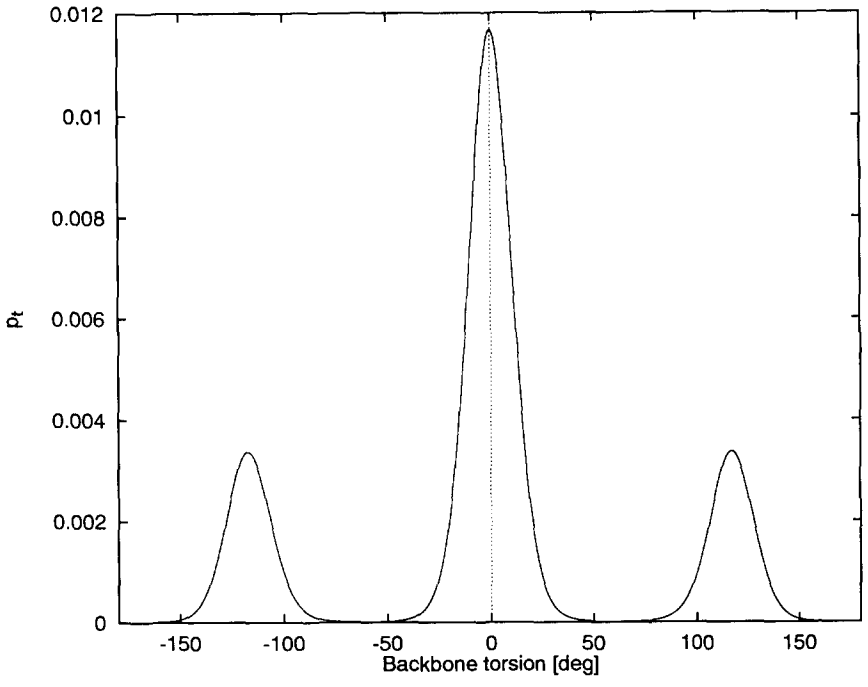

Figure 8 Probability distribution of the PE backbone torsional angles corresponding to the torsional potential of *Figure 7*

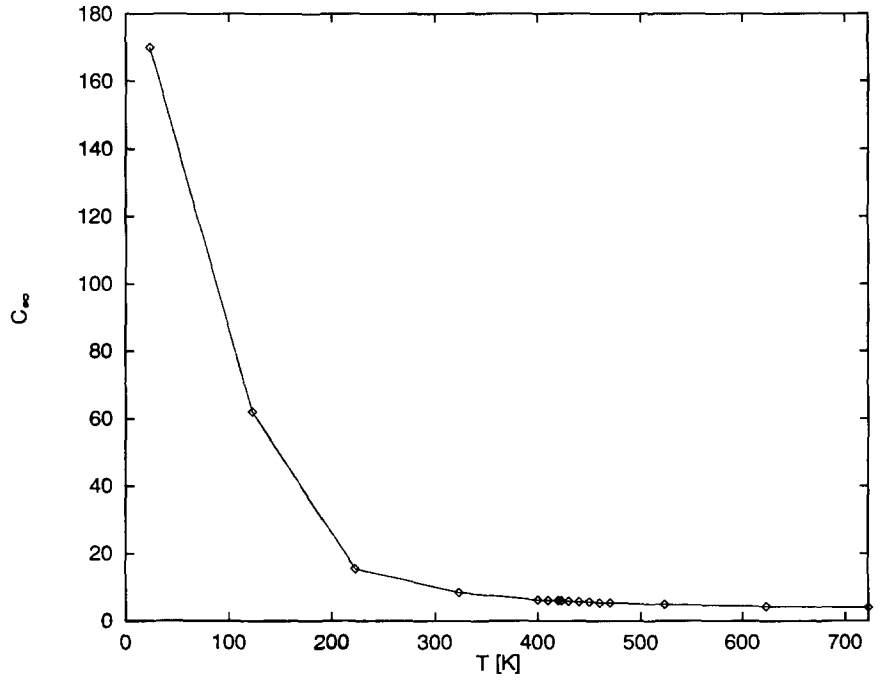

Figure 9 Temperature behaviour of the PE characteristic ratio C_∞ obtained using the force fields developed in this work

chains of PE[25]. As can be seen, the values obtained for the characteristic ratio values in this work are some 7% lower than the accepted experimental values. From the temperature variation of C_∞ in the region 400–500 K we have obtained the temperature coefficient $d\ln(C_\infty)/dT$ by a linear fit of the logarithm of the C_∞ curve limited to that T range. The best-fit value of the temperature coefficient was $d\ln(C_\infty)/dT = 2.3 \times 10^{-3}\,K^{-1}$. This value is slightly higher than the ones reported in the literature[32].

To summarize, we have obtained the constants for a set of force fields that describe completely the local conformation of the chain through comparison of the calculated and experimental neutron structure factors. These same force fields obtained in this exploratory study yield large-scale structures that are in reasonable agreement with published values. The differences between the calculated and experimental values of C_∞ and the temperature coefficient may be related to the exclusion of higher-order dependences within the torsional potential. In essence we have not considered the dependence of the total potential on the state of the neighbouring skeletal bonds. However, given this limitation, the results are most encouraging.

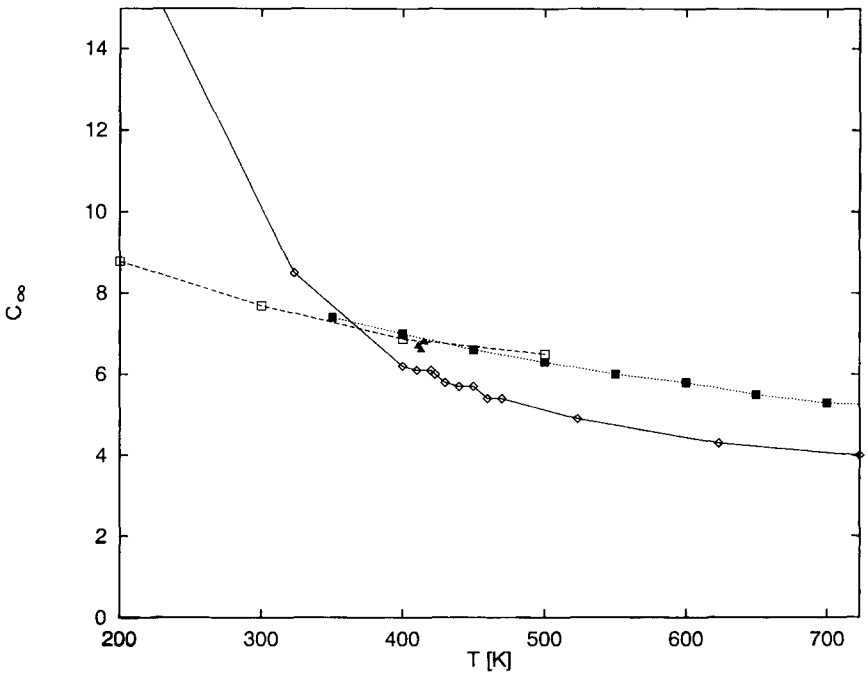

Figure 10 Comparison of our results for C_∞ and literature data: (——) the results using the force fields developed in this work; (....) model calculation by Flory *et al.*[32]; (▲) experimental results from PE in solution[32]; (- - - -) model calculation by Raucci *et al.*[25]

We now turn to the torsional angle potential for PTFE. In a previous study using neutron scattering data from molten PTFE[11], we utilize a model in which the backbone torsional angle distribution was represented, in accordance with the so-called RIS approach, in terms of a limited number of possible rotational isomers and their probabilities of occurrence. This work showed emphatically that the experimental structure factor could be satisfactorily reproduced with four rotational isomers, namely a split *trans* and two *gauche* states. The twisting away of the *trans* state from the planar zig-zag arrangement is ±18°, similar to that found in the crystalline state[14]. The associated probability of a *trans* torsion was found to be 0.86, a value that corresponds to a highly persistent chain conformation. We did not consider the necessity of including a further splitting of the *gauche* states, as proposed by recent model calculations performed on PTFE and based on *ab initio* predictions on small perfluoroalkane molecules[38].

If we consider the expected form of the torsional potential, then the split nature of the minimum in the potential corresponding to the *trans* conformer means that a large number of terms are required to reproduce the potential using equation (7). In fact, tests showed that the features described above could only be reproduced by a cosine power expansion of the torsional energy with a minimum of seven terms. Since in this type of study we are only utilizing the low-energy portion of the potential curve, for this exploratory study we have adopted an alternative functional form that involves fewer terms and is particularly suited to the description of the wells of the torsional potential. First our chosen functional form is based on the probability function. We represent the complete probability function by the superposition of four Gaussian distributions each associated with a well in the potential. The parameters associated with each Gaussian distribution are the position and width of each function (in terms of torsional angle) and the integrated intensities; the probability distribution is normalized to unity. In this function there is a direct link between the resulting distribution of torsional angles and this set of parameters, in contrast to that shown for the functional form of equation (7). The relative torsional potential can be obtained by inverting the procedure for calculating the probability distribution from the torsional potential described in the previous section to enable the calculation of properties over a range of temperatures. We followed the same grid scan procedure to that employed for PE to obtain the five parameters of the Gaussian distribution. We have imposed the condition that the probability distribution and hence the potential are even functions. The resulting probability distribution function has the Gaussians centred at ±16° and ±120°, with associated widths of 13° and 8° and integrated intensities of 0.43 and 0.07 respectively. These can be associated with a split *trans* state and two *gauche* states with a total probability of *trans* torsions of 0.86. *Figure 11* shows the torsional angle distribution for the probability function with these parameters appropriate to the PTFE melt at 623 K. In contrast, calculation of the potential as a function of a skeletal torsion angle using the CHARMm force field fails to predict the splitting of the minimum for the *trans* conformers[11]. The positions of the minima found in the torsional potential obtained in this work are close to those reported by Smith *et al.*[38] on the basis of detailed *ab initio* calculations.

Figure 12 shows the fit of the model defined by the complete refined force field (full curve) to the experimental diffraction data of PTFE (symbols). As a comparison, we also show the scattering curve obtained by a model in which the geometric parameters defining the chain are kept rigid at a fixed value and the torsional potential is described by a single *trans* minimum at 0° (broken curve). Clearly the refinement procedure is very sensitive to the details of the force field used; the second

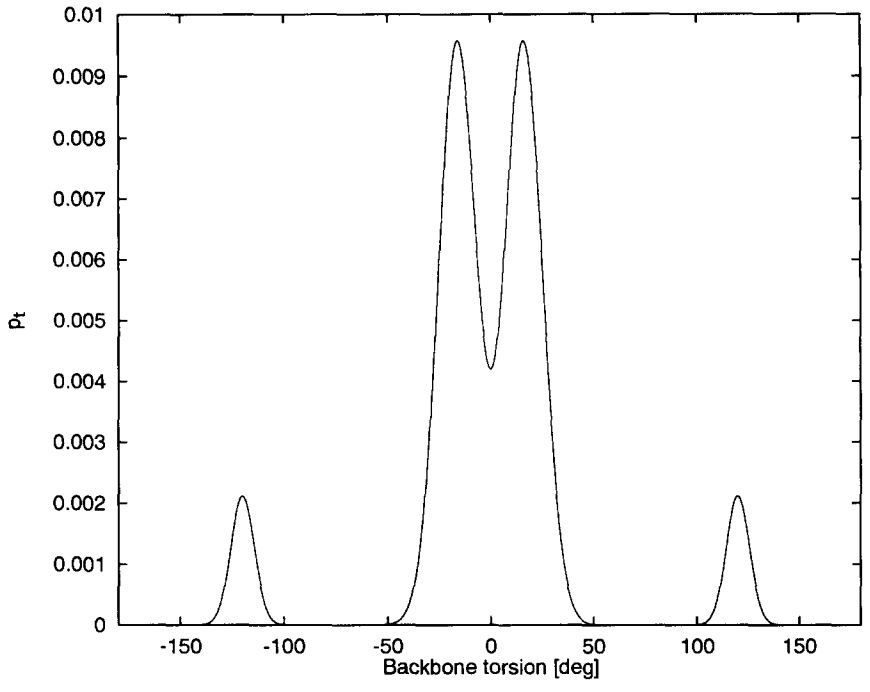

Figure 11 Optimized torsional angle probability distribution obtained for molten PTFE

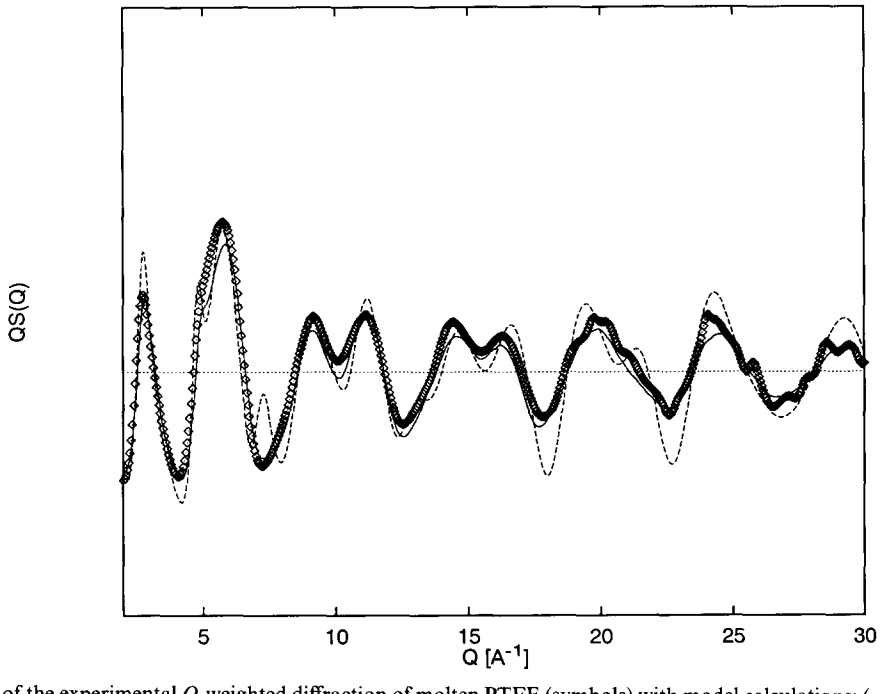

Figure 12 Comparison of the experimental Q-weighted diffraction of molten PTFE (symbols) with model calculations: (——) complete refined force field with distributions of values for the geometric parameters and a torsional potential defined by a split *trans* state; (- - - -) a model in which geometric parameters are set at fixed values and the torsional potential is defined by a non-split *trans* minimum

model is inadequate for the description of the scattering features.

We have utilized the complete force field to predict the temperature behaviour of the characteristic ratio C_∞ and the persistence length q of the PTFE chain. *Figures 13* and *14* show the results obtained for the two quantities respectively.

Problems associated with the insolubility of PTFE at low temperatures have limited the available data on C_∞, and of course the classic approach of deuterium labelling coupled with small-angle neutron scattering to obtain the radius of gyration is not a possibility with PTFE. The two experimental studies of C_∞ to date, namely that of Bates and Stockmayer[39,40] and a more recent light-scattering study[41], yield rather different values of 30 (±15) and 8 (±2.5) for PTFE at 600 K; each is plotted for comparison in *Figure 13*. The values obtained for the characteristic ratio from the force fields derived in this work are substantially lower than that obtained by Bates *et al.* from perfluoroalkanes and closer to that obtained by Chu *et al.* through light-scattering studies on PTFE solutions. It is difficult to

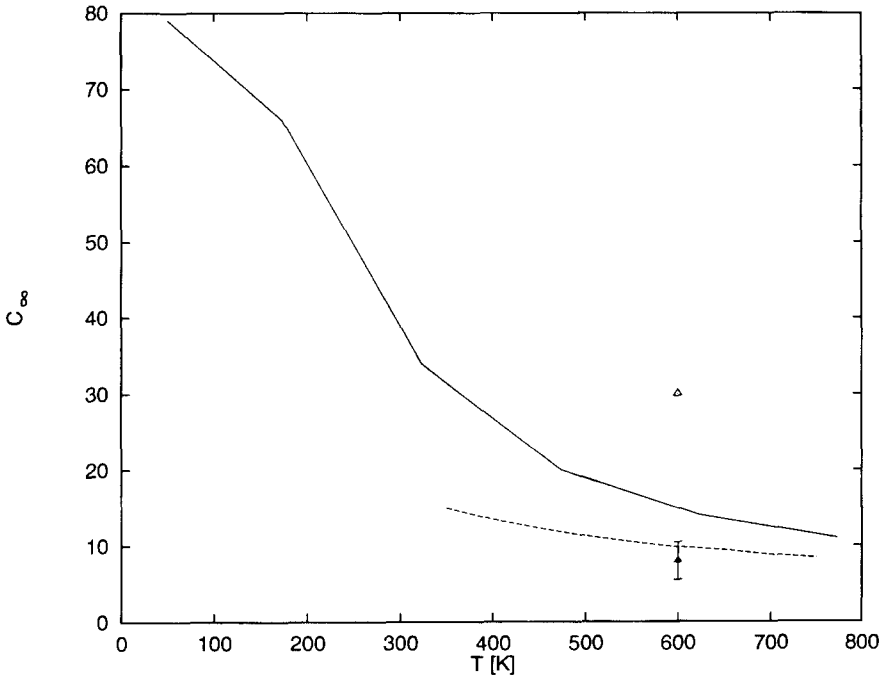

Figure 13 Temperature behaviour of the PTFE characteristic ratio C_∞: (——) the results from our refinement procedure; (- - - -) model calculation by Smith *et al.*[38]; (△) experimental results from perfluroalkanes in solution[39,40]; (▲) experimental results by Chu *et al.*[41]

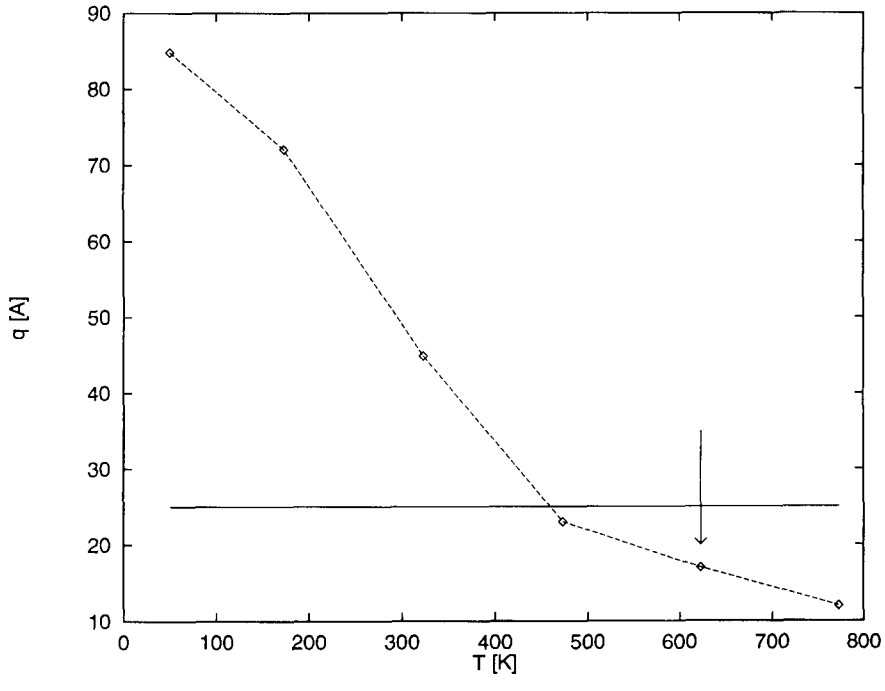

Figure 14 Predicted temperature behaviour of the PTFE persistence length q, obtained from the force fields derived in this work. The arrow indicates the temperature of the experiment, at which the refinement was operated. The solid line represents the threshold q value for liquid crystallinity[43]

assess the uncertainty associated with these light-scattering measurements because little is known about the solvent quality, and the procedure and model employed to convert the radius of gyration value to a characteristic ratio are not given.

Recent calculations of the conformational characteristics of PTFE have been reported that employed a six-state RIS model in which the probabilities are calculated using very comprehensive *ab initio* calculations on model compounds up to perfluoropentane[38]. The results of that RIS model are also plotted in *Figure 13*: these values are also larger than those observed by Chu *et al.*[41].

Our approach to the evaluation of C_∞ is based on a very precise specification of the local conformation and the use of that specification to generate larger-scale structures. In that sense, the approach is very similar to that inherent to theoretical studies in which potential functions or probabilities are based on either *ab initio* or semiempirical calculations. The difference in our work is that the procedure utilizes only experimental data and is

based entirely on polymers. As was emphasized in the case of PE, the functional form of the torsional potential did not allow for the near-neighbour dependence of the probability of a particular torsional angle. However, despite this simplification, the results obtained are very encouraging in terms of the agreement with the neutron scattering structure factor and with the larger-scale properties, and work to consider more general potentials is in progress.

It is interesting to compare the variation of C_∞ for PE and PTFE over a large temperature range. The split nature of the potential around the minimum corresponding to the *trans* conformer of PTFE leads to a less extended chain at lower temperatures than that calculated for PE. In fact there is a relatively sharp transition in the values of C_∞ between the two types of chain configuration at a particular temperature as the offset angle for the *trans* conformer is varied. This behaviour contrasts that observed at higher temperatures, where it is the population of high-energy defects that dominates the value of C_∞ and leads to lower values for PE in comparison to PTFE. These features serve to emphasize the importance of the detail of force fields if useful predictions of both structure and properties of polymers are to be made.

There has been speculation in the past that the apparent 'stiffness' of the PTFE chain might result in the formation of a liquid-crystal phase. Some previous reports[32,42] have placed PTFE at the borderline of isotropic/liquid-crystal behaviour. *Figure 14* shows the predicted temperature dependence of the persistence length for molten PTFE evaluated with the force field derived in this work. A measure of the stiffness of the chain is given by the chain anisotropy factor, namely the ratio between persistence length and chain diameter. At the temperature of measurement, namely 623 K, the chain anisotropy factor is 3.4, indicating a very stiff chain but remaining below the predicted boundary between anisotropic melt and liquid-crystalline order[43].

The horizontal solid line in *Figure 14* represents the q value at which a macromolecular system is expected to exhibit liquid-crystalline behaviour based on a critical value of the chain anisotropy factor of 5[43]. The crossover between this threshold value and the predicted q curve for PTFE occurs, as can be seen, at $T = 460$ K, which is within the crystalline phase.

CONCLUSIONS

This exploratory study has shown the viability of broad-Q neutron scattering tightly coupled to computer modelling for the extraction of potentials suitable for a realistic description of polymer chains in the molten state. The potential of the system has been split into different non-interacting terms referring to bond stretching, angle bending and torsional rotation respectively. The torsional potential includes all interactions, including those conventionally separated as non-bonded and electrostatic terms. In effect it includes the contributions from the neighbouring chain segments in addition to the intramolecular component. If the Flory postulate is correct, then the torsional potential refers to a single chain; otherwise these force fields are specific to the particular polymer and to the molten state of that polymer. We have utilized a grid scan procedure with a variable spacing to determine the relevant force-field parameters directly from the experimental neutron diffraction data. The technique, applied to molten PE and PTFE, has provided a wealth of detailed and accurate information on the polymers. Since the potential is derived directly from experimental evidence, it is realistic at least in terms of the local conformation. Calculation of the larger-scale properties of PE and PTFE chains confirms the appropriateness of these force fields. The force fields derived are somewhat simplified by the inclusion of non-bonded interactions in the torsional potential and by the lack of near-neighbour correlations in terms of torsion angles within the torsional potential. These deliberate simplifications hamper the transferability of this potential to other polymer systems. Nevertheless, our main aim was the assessment of the feasibility of our neutron scattering and modelling approach for the study and validation of force-field expressions in general; the fact that the results obtained with our procedure are reasonable demonstrates that the procedure is indeed viable. We believe that this approach holds a great potential in its applicability to more general and complete force fields describing various disordered polymer systems, and it certainly underlines the value of this type of study in validating existing force fields.

ACKNOWLEDGEMENTS

This work is supported by the Engineering and Physical Science Research Council (GR/H66907) and by Molecular Simulations.

REFERENCES

1 Baumgartner, A. and Binder, K. *J. Chem. Phys.* 1979, **71**, 2541
2 Binder, K. and Heermann, D. W. 'Monte Carlo Simulation in Statistical Physics: An Introduction', Springer, Berlin, 1988
3 Paul, W., Binder, K., Heermann, D. W. and Kremer, K. *J. Phys. Paris (II)* 1991, **37**, 1
4 Paul, W., Binder, K., Heermann, D. W. and Kremer, K. *J. Chem. Phys.* 1991, **37**, 7726
5 Theodorou, D. N. and Suter, U. W. *Macromolecules* 1986, **19**, 139
6 Theodorou, D. N. and Suter, U. W. *Macromolecules* 1986, **19**, 379
7 Mott, P. H., Argon, A. S. and Suter, U. W. *Polym. Prepr.* 1989, **30**, 34
8 Brown, D. and Clarke, J. H. R. *Macromolecules* 1991, **24**, 2075
9 Sun, H., Mumby, S. J., Maple, J. R. and Hagler, A. T. *J. Am. Chem. Soc.* 1993, **116**, 2978
10 Sun, H. *J. Comput. Chem.* 1994, **15**, 752
11 Rosi-Schwartz, B. and Mitchell, G. R., *Polymer* 1994, **35**, 3139
12 Rosi-Schwartz, B. and Mitchell, G. R. *Nucl. Instrum. Meth. (A)* 1995, **354**, 17
13 Bunn, C. W. and Howells, E. R. *Nature* 1954, **174**, 549
14 De Rosa, C., Guerra, G., Petraccone, V., Centore, R. and Corradini, P. *Macromolecules* 1988, **21**, 1174
15 Steele, D. *J. Chem. Soc., Faraday Trans. (II)* 1985, **81**, 1077
16 Rigby, D. and Roe, R. J. *Macromolecules* 1989, **22**, 2259
17 Ryckaert, J. P. in 'Computer Modelling of Fluids, Polymers and Solids' (Eds. C. R. A. Catlow, S. C. Parker and M. P. Allen), Kluwer Academic, London, 1990, p.189
18 Dillen, J. L. M. *J. Comput. Chem.* 1995, **16**, 595
19 Mitchell, G. R. in 'Order in the Amorphous "State" of Polymers' (Eds. S. E. Keinath, R. L. Miller and J. K. Rieke), Plenum, New York, 1987, p.1
20 Mitchell, G. R. in 'Comprehensive Polymer Science' (Eds. G. Allen, J. C. Bevington, C. Booth and C. Price), Pergamon, Oxford, 1989, Vol.I, Ch.31, p.687

21 Mitchell, G. R., MESA User Guide, J. J. Thomson Physical Laboratory, University of Reading, 1995
22 Rosi-Schwartz, B. and Mitchell, G. R. *Polymer* 1994, **35**, 5398
23 Weber, T. A. *J. Chem. Phys.* 1978, **69**, 2347
24 van der Ploeg, P. and Berendsen, H. J. C. *J. Chem. Phys.* 1982, **76**, 3271
25 Raucci, R. and Vacatello, M. *Makromol. Chem., Theor. Simul.* 1993, **2**, 875
26 Molecular Simulations, CHARMm User Guide, Molecular Simulations Inc., 1988
27 Weiner, P. K. and Kollman, P. A. *J. Comput. Chem.* 1981, **2**, 287
28 Dinur, U. and Hagler, A. T. *J. Am. Chem. Soc.* 1989, **111**, 5149
29 Habenschuss, A. and Narten, A. H. *J. Chem. Phys.* 1990, **92**, 5692
30 Misawa, M., Kanaya, T. and Fukunaga, T. *J. Chem. Phys.* 1991, **94**, 8413
31 Stewart, J. J. P. *J. Comput. Aided Mol. Design.* 1990, **4**, 1
32 Flory, P. J. 'Statistical Mechanics of Chain Molecules', Wiley, New York, 1969
33 Mattice, W. L. and Suter, U. W. 'Conformational Theory of Large Molecules', Wiley, New York, 1994
34 Cook, R. and Moon, M. *Macromolecules* 1978, **11**, 1054
35 Cook, R. and Moon, M. *Macromolecules* 1980, **13**, 1537
36 Mitchell, G. R., Lovell, R. and Windle, A. H. *Polymer* 1982, **23**, 1273
37 Lieser, G., Fishcer, E. W. and Ibel, K. *J. Polym. Sci., Polym. Lett. Edn.* 1975, **13**, 39
38 Smith, G. D., Jaffe, R. L. and Yoon, D. Y. *Macromolecules* 1994, **27**, 3166
39 Bates, T. W. and Stockmayer, W. H. *Macromolecules* 1968, **1**, 12
40 Bates, T. W. and Stockmayer, W. H. *Macromolecules* 1968, **1**, 17
41 Chu, B., Wu, C. and Buck, W. *Macromolecules* 1989, **22**, 831
42 Ronca, G. and Yoon, D. Y. *J. Chem. Phys.* 1982, **76**, 3295
43 Bedford, S. E., Yu, K. and Windle, A. H. *J. Chem. Soc., Faraday Trans.* 1992, **88**, 1765